Size effect on strength of Fiber-Reinforced Self-Compacting Concrete (SCC) after exposure to high temperatures

M. Eren Gülşan[*1], Khamees N. Abdulhaleem[1,2a], Ahmet E. Kurtoğlu[3b] and Abdulkadir Çevik[1c]

[1]*Department of Civil Engineering, Gaziantep University, Gaziantep, Turkey*
[2]*Department of Civil Engineering, Kirkuk University, Kirkuk, Iraq*
[3]*Department of Civil Engineering, Istanbul Gelisim University, Istanbul, Turkey*

Abstract. This pioneer study investigates the size effect on the compressive and tensile strengths of fiber-reinforced self-compacting concrete (FR-SCC) with different specimens, before and after exposure to elevated temperatures. 432 self-compacting concrete (SCC) specimens with two concrete grades (50 and 80 MPa) and three steel fiber ratios (0%, 0.5% and 1%) were prepared and tested. Moreover, based on the experimental results, new formulations were proposed to predict the residual strengths for different specimens. A parametric study was also carried out to investigate the accuracy of proposed formulations. Residual strength results showed that the cylinder specimen with dimensions of 100×200 mm was the most affected, while the cube with a size of 100 mm maintained a constant difference with the standard cylinder (150×300 mm). Temperature effect on the cube specimen (150 mm) was the least in comparison to other specimen sizes and types. In general, provision of steel fibers in SCC mixtures resulted in a reduction in temperature effect on the variance of a conversion factor. Parametric study results confirm that the proposed numerical models are safe to be used for all types of SCC specimens.

Keywords: self-compacting concrete; elevated temperatures; fiber-reinforced; size effect; compressive and tensile strengths

1. Introduction

Compressive and tensile strengths of concrete are the most important mechanical properties in the design of concrete structures, which are routinely specified and tested by control specimens (Nikbin *et al.* 2014). Several international standards and codes recommend various geometries and shapes of test specimens. Most common shapes are the cylinder with dimensions of 150×300 mm and the cube with dimensions of 150 mm. These specimens are known as the standard specimens. Dehestani *et al.* (2014) introduced the relation between the strengths of different specimens and noted that the cubic specimen has higher strength than the cylindrical specimen. Yi *et al.* (2006) proved that the strength ratio of the cube to the cylinder decreases as the concrete grade increases. In general, the concrete strength decreases with the increase in specimen size (Del Viso *et al.* 2007, Kourkoulis and Ganniari-Papageorgiou 2010), and the decrement rate remains nearly constant beyond a certain size limit (Yi *et al.*

2006, Del Viso *et al.* 2007, Sim *et al.* 2013). Van Der Vurst *et al.* (2014) indicated that the higher uniformity in the distribution of stresses causes a reduction in the maximum stresses in the specimen. Yi *et al.* (2006) described the effect of shape and size of the specimen, as well as placement direction on compressive strength based on fracture mechanics. Aslani *et al.* (2017) investigated the effect of shape, size and mould type on the compressive strength of concrete. Maia and Aslani (2016) proposed that modulus of elasticity of the concrete produced from basaltic aggregate was not affected by the specimen geometry.

Self-compacting concrete (SCC) has been widely used in industrial structures throughout the world since it has the ability to flow and fill all sections of forms with little or no vibration as well as prevention of bleeding or segregation (Aslani 2015a, Aslani and Maia 2013). Furthermore, fiber-reinforced SCC (FR-SCC) can be used as a high-performance building materials that combines the benefits of fresh properties of SCC as well as improving the characteristics of the concrete in the hardened state due to adding fibers (Aslani and Nejadi 2013, Aslani and Natoori 2013, Aslani and Bastami 2015).

Fire is one of the most severe risks to a building or structure. A research related with the temperature effect on different concrete specimen types gives an indication regarding the influence extent for each specimen type under the same conditions. Therefore, the mechanical performance of concrete structural members with different shaped and sized cross-sections can be predicted when exposed to elevated temperatures during a possible fire. Due to development of new types of concrete, thermal performance

*Corresponding author, Assistant Professor
  E-mail: gulsan@gantep.edu.tr
[a]Ph.D. Candidate
  E-mail: khamees.abdulhaleem@mail2.gantep.edu.tr
[b]Assistant Professor
  E-mail: aekurtoglu@gelisim.edu.tr
[c]Professor
  E-mail: akcevik@gantep.edu.tr

Table 1 Chemical analysis of cement and binder contents

Oxide (%)	Cement	Fly ash	Silica fume
SiO_2	20.4	56.2	93.2
Fe_2O_3	3.9	6.69	1.5
CaO	63.0	4.24	0.4
Al_2O_3	4.9	20.17	0.7
MgO	1.7	1.92	0.1
SO_3	2.0	0.49	0.1
$Na_2O + K_2O$	0.9	2.36	1.4

Table 2 Properties of fibers used in the study

Properties	Steel Fiber (SF)	Polypropylene fiber (PP)
Length (mm)	30	12
Diameter (mm)	0.75	0.02
Density (g/cm^3)	7.8	0.91
Tensile strength (MPa)	1200	450

of them has been investigated by several investigations. For instance, Aslani (2015b) investigated the mechanical performance of geopolymer concrete at elevated temperatures. Sideris (2007) has shown that the strength retention level in SCC is higher than in conventional concrete (CC) and SCC exhibits higher strength even at high temperatures. Bamonte and Gambarova (2016) have proposed that even the strength of SCC is superior to normal concrete, it is more sensitive to spalling at elevated temperatures. Numerous studies focusing on the mechanical properties of SCC at room temperature are also available in the literature. However, there are comparatively few studies regarding mechanical behavior of SCC and FR-SCC at elevated temperatures which had been achieved by several researchers (Aslani and Bastami 2011, Aslani 2013b, Aslani and Samali 2013b, Bastami *et al*. 2014, Aslani and Samali 2013a). Moreover, no study, as of yet, has investigated the size effect on the mechanical properties (tensile and compressive strengths) of different FR-SCC specimens after exposure to elevated temperatures. There is only one research related with effect of specimen size on mechanical properties of SCC which was achieved by Aslani (2013a). He carried out an experimental study regarding the effect of size and shape of common specimens on compressive and tensile strengths of SCC with and without fibers at room temperature based on fracture mechanics.

In this study, an experimental program was implemented to examine the size effect (size and shape of the specimen)

on compressive and tensile strengths of FR-SCC before and after exposure to elevated temperatures for the first time in literature. To this end, 432 cubic and cylindrical specimens of different sizes were prepared. Additionally, numerical models were developed to obtain the residual compressive and tensile strengths for common specimens of FR-SCC after exposure to elevated temperatures.

2. Experimental program

A total of six SCC mixtures were prepared for each desired temperature as follows: two concrete grades (50 MPa and 80 MPa) and three steel fiber (SF) ratios of 0%, 0.5% and 1%. Each mixture contained polypropylene fiber (PP) with volume fraction of 0.1%. The specimens were casted and tested at room temperature, and after exposure to elevated temperatures of 250, 500, and 750℃.

2.1 Material characteristics

Portland cement (ASTM type II) with specific gravity of 3.12 and fineness of 295 m^2/kg was used in all mixtures. Locally available crushed stone and crushed sand (from the same source) with a specific gravity of 2.65 were used as coarse and fine aggregate, and contained water absorptions of 0.8% and 1.4%, respectively. The maximum aggregate size was 11 mm. To satisfy the SCC requirements, fly ash (type F) and silica fume were used as binder additives in concrete mixtures. The chemical compositions of cement, fly ash, and silica fume are presented in Table 1. A high-

Table 3 Mix proportions of SCC mixtures

Materials	Mix code					
	FR-MSCC			FR-HSCC		
	FR-MSCC-S0	FR-MSCC-S5	FR-MSCC-S10	FR-HSCC-S0	FR-HSCC-S5	FR-HSCC-S10
Cement (kg/m^3)		250			450	
Fine Aggregate (kg/m^3)		1100			1100	
Coarse Aggregate (kg/m^3)		700			700	
Fly ash (kg/m^3)		215			50	
Silica fume (kg/m^3)		35			35	
Water (l/m^3)		170			160	
Super-plasticizer (% volume of binder)		1.0			1.2	
Steel fiber (SF) (kg/m^3)	0	39	78	0	39	78
Polypropylene fiber (PP) (kg/m^3)		0.91			0.91	
w/c[*]		0.68			0.36	
w/(c+b)[*]		0.34			0.30	

*w/c=water/cement ratio, w/b=water/binder ratio, binder content=cement+fly ash+silica fume.

performance super-plasticizer was added to the mixture to obtain the required workability for the fiber-reinforced self-compacting concrete used. Hooked-end steel fiber (SF) and polypropylene fiber (PP) were used to produce FR-SCC. The properties of the SF and PP fibers utilized in the study are shown in Table 2 and the proportions of FR-SCC mixtures are listed in Table 3.

2.2 Classification of mixtures

Classification of mixtures is based on their compressive strength class and the SF ratio as shown in Table 3. The first two letters (FR) denote that the mixture contains 0.1% of PP fibers while the compressive strength class is represented by M for medium strength and H for high strength, followed by the SCC abbreviation of self-compacting concrete, and finally the steel fiber (SF) volume fraction. For example, FR-HSCC-S10 refers to a high-strength SCC mix with an SF ratio of 1%.

Six mixtures were prepared for each desired temperature, resulting in 24 mixtures in total. Each batch included eighteen specimens composed of six cylinders with dimensions of 150×300 mm (S-150), six cylinders with dimensions of 100×200 mm (S-100), three cubes with sizes of 100 mm (C-100), and three cubes with sizes of 150 mm (C-150). All measurements are taken as the average of three readings.

3. Testing procedure

3.1 Fresh properties testing

L-box, V-funnel, and Slump flow tests were carried out to determine the fresh properties of considered mixtures. Fresh test results of produced mixtures are listed in Table 4. The fresh test results of the mixtures were found to be within the range recommended by EFNARC (2005). As expected, presence of fibers has a negative effect on the workability and thus leads to higher flow time.

3.2 Heating regime

After the 28±1 days of water curing process, the specimens (for one batch) were left in the laboratory for 24 hours to dry before placing into the electric furnace.

After heating with rate of 5 °C/min to desited temperature, the speciments were naturally cooled down to room temperature for 24 hours prior to loading test.

3.3 Loading test

Cubic (C-100 and C-150) and cylindrical (S-100 and S-150) specimens were tested in a universal testing machine with 3000 kN capacity. Compressive strength was determined in accordance with ASTM (2004) and B.S (2000) standards for cylindrical and cubic specimens, respectively. According to the specification, the loading rate for C-100, C-150, S-100 and S-150 are 2, 4.5, 1.5 and 3.5 N/s, respectively. Splitting tensile test was performed on two different sizes of cylindrical specimens (S-100 and S-

Table 4 Fresh properties of FR-SCC mixtures

Specimen	SF ratio (%)	Slump-flow (mm)	T500 mm (s)	V-funnel flow (s)	Blocking ratio (H_2/H_1)
FR-MSCC-S0	0	700	2.62	8.22	0.93
FR-MSCC-S5	0.5	665	3.45	14.64	0.87
FR-MSCC-S10	1.0	610	4.34	19.16	0.83
FR-HSCC-S0	0	670	3.17	12.71	0.88
FR-HSCC-S5	0.5	615	4.10	18.54	0.83
FR-HSCC-S10	1.0	570	4.92	23.87	0.80
Limitation EFNARC (SF1)		520-700	2-5	≤ 12	0.8-1

Table 5 Compressive strength of FR-MSCC specimens after exposure to different temperatures

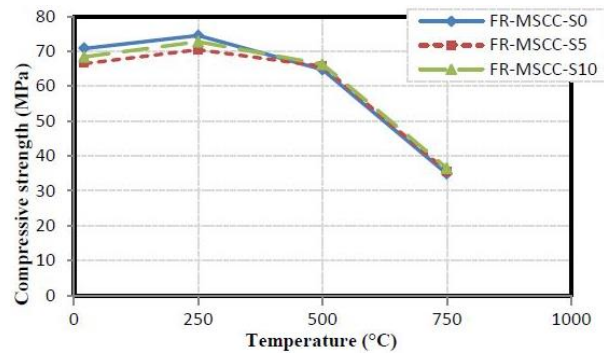| Mixture	Specimen	Compressive strength at room temperature (MPa)	Residual strength (%) after exposure to elevated temperature		
			250°C	500°C	750°C
FR-MSCC-S0	C-100	**70.83**	105	91	49
	C-150	**67.15**	96	91	62
	S-100	**55.59**	94	71	32
	S-150	**52.94**	101	92	40
FR-MSCC-S5	C-100	**66.48**	106	99	53
	C-150	**63.67**	106	97	69
	S-100	**52.79**	108	81	39
	S-150	**51.03**	107	99	50
FR-MSCC-S10	C-100	**68.42**	106	97	53
	C-150	**64.57**	105	98	74
	S-100	**53.81**	110	80	40
	S-150	**50.78**	108	97	53

150) and was conducted as per ASTM (2004). S-100 and S-150 cylinder specimens were loaded with a rate of 1.0 and 1.5 kN/s, respectively, for splitting tensile strength test. Test results represent the average of three readings for corresponding measurements of each specimen.

4. Results and discussion

4.1 Compressive strength

In general, the increment in temperature level resulted in lower compressive strength for FR-SCC specimens. However, a slight increase in compressive strength was recorded for FR-SCC specimens after exposure to 250°C. This can be attributed to the re-hydration of concrete paste induced to combine water migration in the pores (Fares *et al.* 2010, Dias *et al.* 1990). Thereafter, rise in temperature resulted in higher thermal expansion difference and, water evaporation increased pore pressure, leading to a significant reduction in compressive strength (Zhang and Bicanic, 2002). The compressive strength dropped abruptly after exposure to temperatures higher than 500°C.
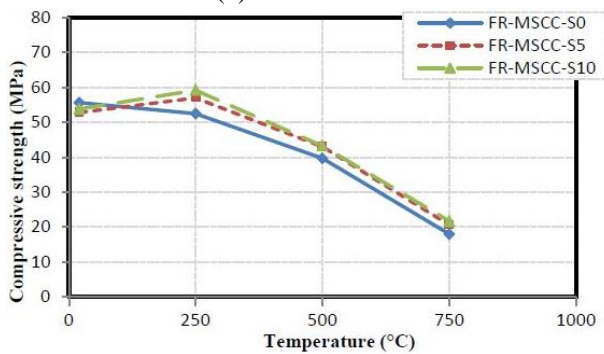
No explosive spalling was observed at each temperature for any SCC specimens, which is attributable to the
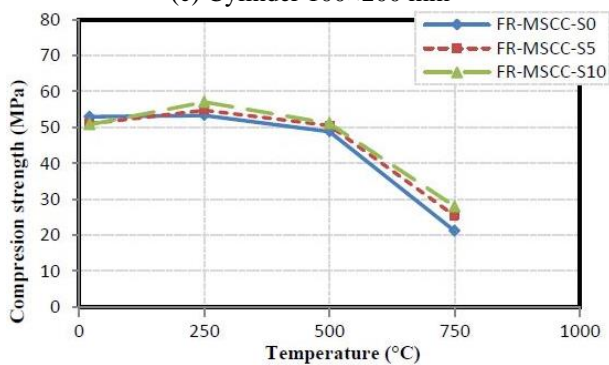
(a) Cube 100 mm
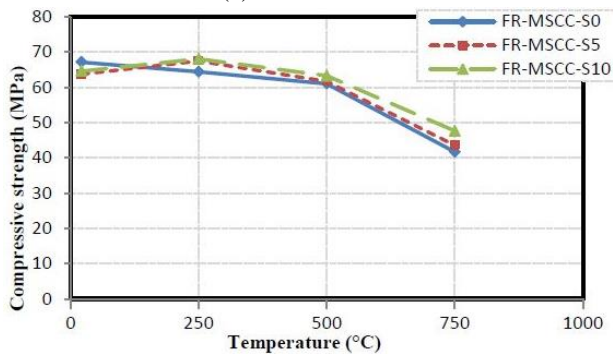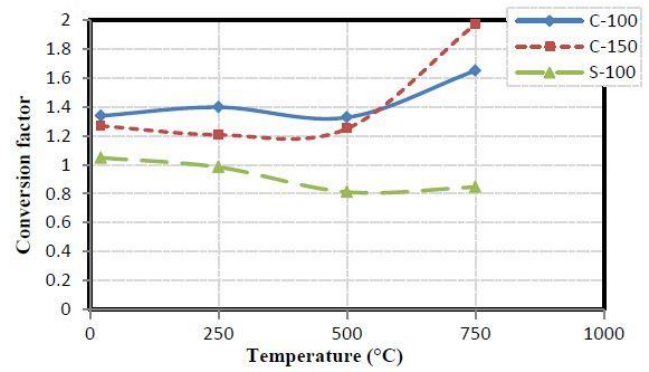

(b) Cube 150 mm

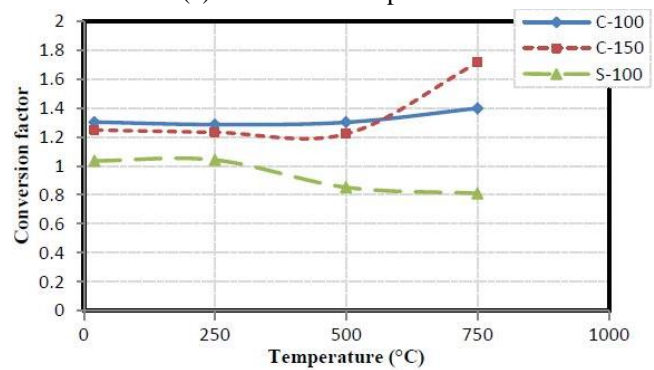(c) Cylinder 100×200 mm

(d) Cylinder 150×300 mm

Fig. 1 Compressive strength of FR-MSCC specimens before and after exposure to elevated temperatures

(a) FR-MSCC-S0 specimens

(b) FR-MSCC-S5 specimens
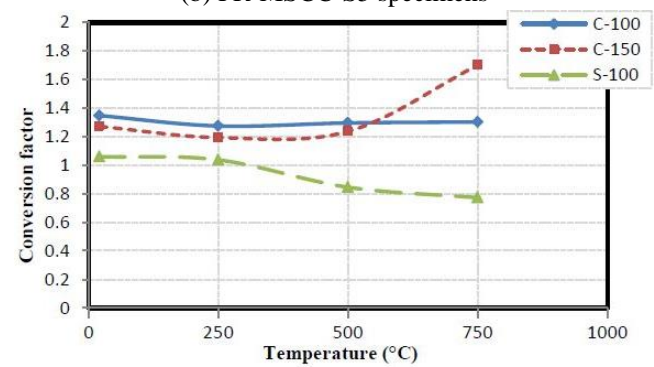
(c) FR-MSCC-S10 specimens

Fig. 2 Conversion factor for FR-MSCC specimens before and after exposure to elevated temperatures

presence of polypropylene fibers (PP). Provision of steel fibers (SF) improved the residual strength of FR-SCC specimens after exposure to elevated temperatures.

4.1.1 Medium strength self-compacting concrete (FR-MSCC)

Table 5 and Fig. 1 show the compressive strength of fiber-reinforced medium strength self-compacting concrete (FR-MSCC), with and without steel fiber for cubic and cylindrical specimens before and after exposure to elevated temperatures. For the specimen of the same shape, the temperature effect increased as specimen size decreased. After exposure to 750°C, the residual strength of the large cylinder (S-150) decreased by 52%, whereas the small cube maintained 52% of its strength at room temperature. After exposure to temperatures higher than 250°C, strength of small cylinder (S-100) suffered a reduction greater than the other specimens, whereas large cube (C-150) was least affected at elevated temperature. The cylindrical specimens were more responsive to steel fibers as compared to cubic specimens. However, the residual compressive strength of cubic specimens was higher than that of the cylindrical specimens. This can be attributed to the fact that the

temperature transfer from the surface to the center of a cylindrical specimen was easier as compared to cubic specimens. Therefore, the distribution of temperature is more symmetrical and homogeneous in cylindrical specimens. For this reason, sensitivity of the cylindrical specimens when exposed to elevated temperatures is higher.

Conversion factor

Conversion factor was calculated based on the test results. It represents the compressive strength ratio between the different specimens (C-100, C-150 and S-100) and the standard specimen (S-150) as shown in Fig. 2.

Although the small cube (C-100) kept a fixed ratio, the difference in the conversion factor for the other specimens increased as the temperature rose. After exposure to 750°C, the conversion factor for the small cylinder decreased by 22%, whereas it was nearly 42% higher for the large cube at room temperature. The addition of steel fiber to FR-MSCC mixtures contributed to a reduction in the variation of conversion factor for the concrete specimen particularly for the small cube (C-100).

4.1.2 High strength self compacting concrete (FR-HSCC)

The compressive strength of fiber-reinforced high strength self-compacting concrete (FR-HSCC) for the specimens before and after exposure to elevated temperatures is shown in Fig. 3 and Table 6. After FR-HSCC specimens without steel fibers were exposed to 750°C, large cube had a significant residual strength while the large cylinder suffered a higher loss in compressive strength.

Considering the improvement in residual strength with respect to the amount of steel fiber, it was observed that the small cylinder yielded best performance, while the small cube affected after exposure to 750°C. In general, the addition of 1% steel fiber to SCC mixtures improved the residual strength of cylindrical specimens as much as 3 times as compared to cubic specimens as shown in Table 6.

Conversion factor

Fig. 4 shows the conversion factor for FR-HSCC specimens with and without steel fibers, before and after exposure to elevated temperatures. The conversion factor for the small cylinder maintained almost constant after exposure to elevated temperatures. The addition of 1% steel fiber reduced the variance of conversion factor for cubic specimens nearly 20% after exposure to 750°C. In general, variation of conversion factor decreased as the concrete grade increased for the same specimen after exposure to elevated temperatures. Also, presence of steel fibers in FR-HSCC mixtures contributed to a reduction in temperature effect on the variation of a conversion factor.

4.2 Tensile strength

Tensile strength of FR-SCC with and without steel fiber before and after elevated temperatures is shown in Fig. 6, Table 7 and Table 8 for the small and large cylinders. It was

(a) Cube 100 mm

(b) Cube 150 mm
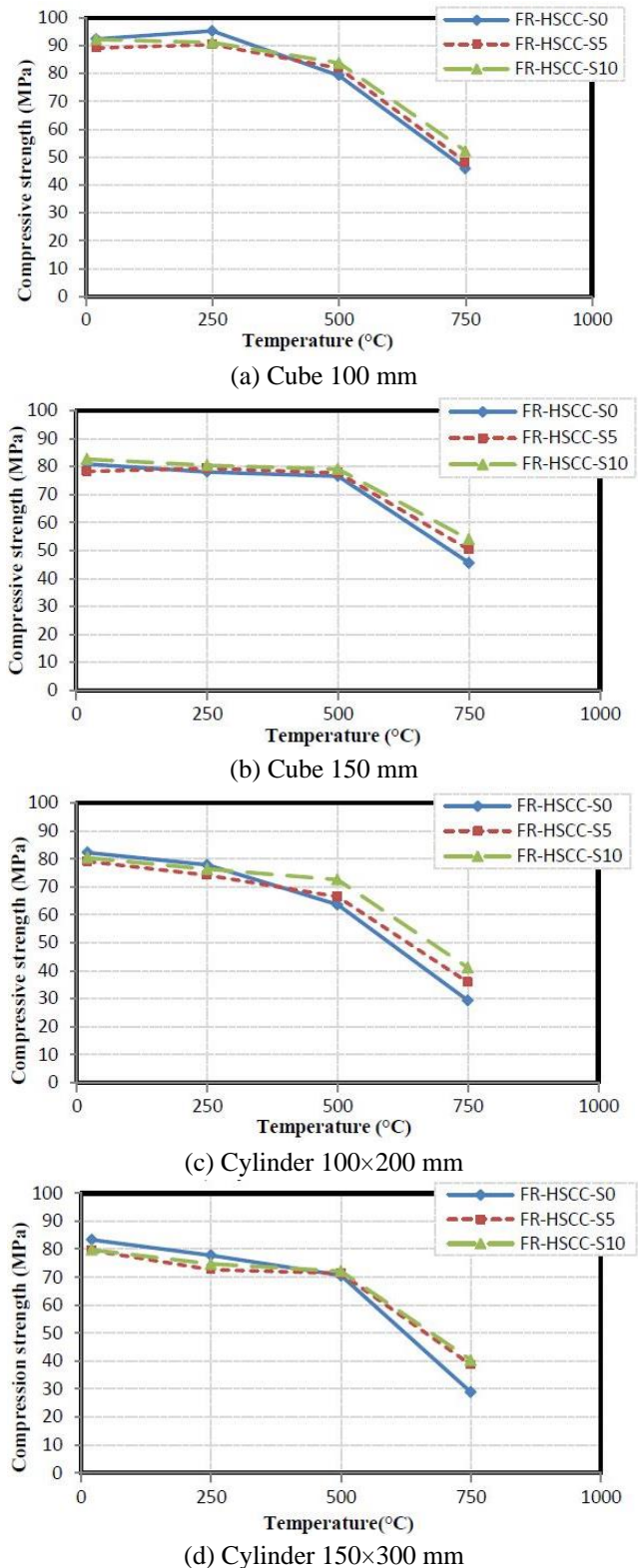
(c) Cylinder 100×200 mm

(d) Cylinder 150×300 mm

Fig. 3 Compressive strength of FR-HSCC specimens before and after exposure to elevated temperatures

observed that small cylinder (S-100) affected more than the large one (S-150) when exposed to elevated temperatures. Reduction in strength of small cylinder was much faster than the strength loss of the large cylinder after exposure to elevated temperatures, as shown in Table 7 and Table 8. It
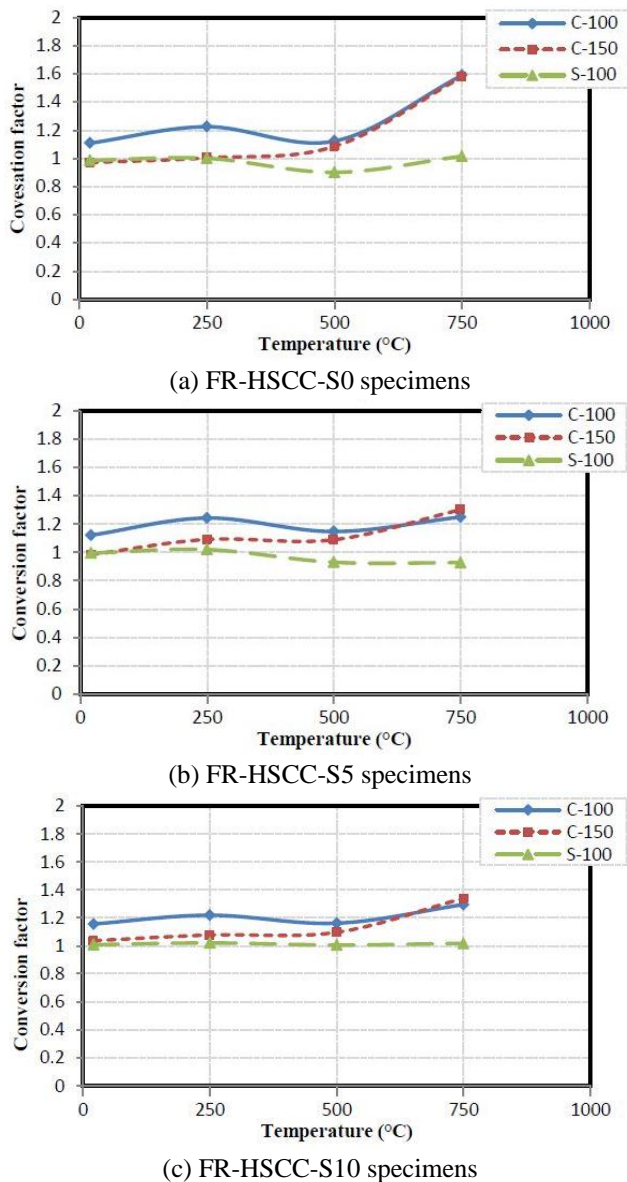
(a) FR-HSCC-S0 specimens

(b) FR-HSCC-S5 specimens

(c) FR-HSCC-S10 specimens

Fig. 4 Conversion factor for FR-MSCC specimens before and after exposure to elevated temperatures

FR-HSCC-S0 FR-HSCC-S5 FR-HSCC-S10

Fig. 5 Shape of failure for different FR-SCC specimens under compression test, after exposure to temperature 750°C

Table 6 Compressive strength of FR-HSCC specimens after exposure to different temperatures

Mixture	Specimen	Compressive strength at room temperature (MPa)	Residual strength (%) after exposure to elevated temperature		
			250°C	500°C	750°C
FR-HSCC-S0	C-100	**92.43**	103	86	50
	C-150	**80.95**	97	95	56
	S-100	**82.24**	95	77	36
	S-150	**83.36**	93	85	35
FR-HSCC-S5	C-100	**89.19**	101	92	54
	C-150	**78.3**	101	99	64
	S-100	**79.13**	94	84	45
	S-150	**79.49**	92	90	49
FR-HSCC-S10	C-100	**92.23**	99	91	57
	C-150	**82.71**	97	96	65
	S-100	**80.43**	95	90	51
	S-150	**79.78**	94	90	50

Table 7 Tensile strength of FR-MSCC specimens after exposure to different temperatures

Mixture	Specimen	Tensile strength at room temperature (MPa)	Residual strength (%) after exposure to elevated temperature		
			250°C	500°C	750°C
FR-MSCC-S0	S-100	**4.94**	91	68	32
	S-150	**4.55**	85	82	36
FR-MSCC-S5	S-100	**6.48**	98	70	38
	S-150	**6.37**	104	82	45
FR-MSCC-S10	S-100	**6.8**	115	92	44
	S-150	**6.3**	107	91	48

was observed that the determination of tensile strength of FR-SCC large cylinder (standard specimen) is more reliable, particularly when the risk of high temperatures is a concern.

4.3 Comparison of the experimental results with the proposed models

In this part of the study, experimental results obtained from the study are compared with the proposed models in literature. Results of 150×300 mm specimens are used for comparison, since the models are proposed based on this standard specimen. Compressive and tensile strength results of the SCC specimens at room temperature are compared with the models proposed by Aslani and Natoori (2013) in Fig. 7. Moreover, compressive and tensile strength results of SCC specimens after elevated temperatures were compared with several corresponding proposed numerical models (Aslani and Samali 2013a, Aslani 2013b, Aslani and Samali 2013b, Bastami *et al.* 2014) as shown in Fig. 8.
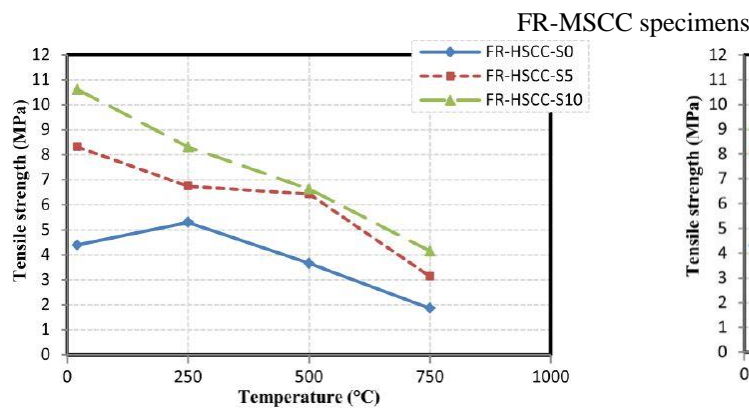
In general a good agreement is observed regarding compressive strength results of the specimens at room
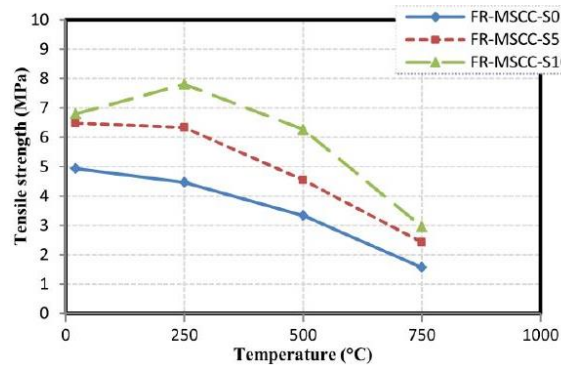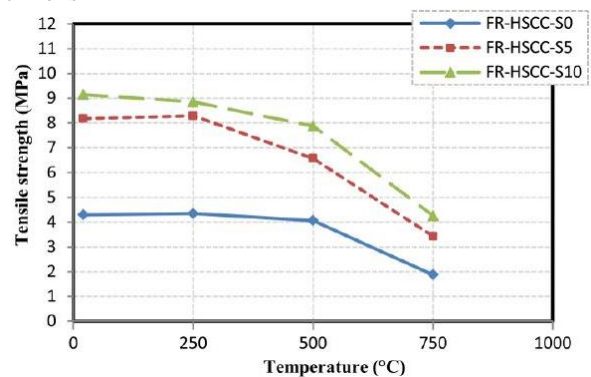
(a) Cylinder 100×200 mm
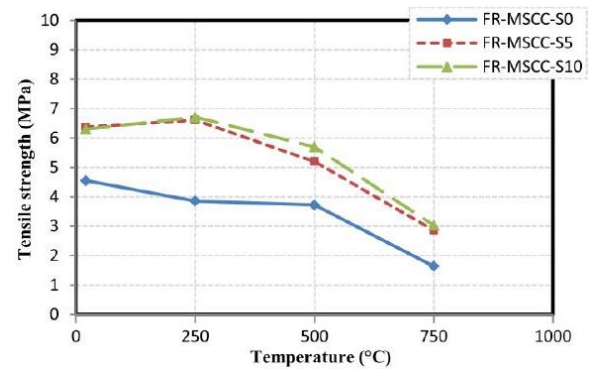
(b) Cylinder 150×300 mm
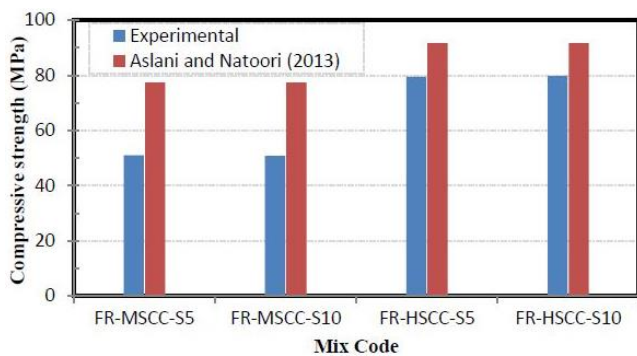
FR-MSCC specimens

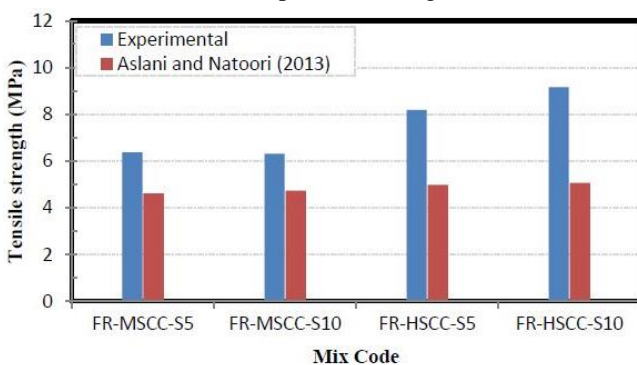(c) Cylinder 100×200 mm

(d) Cylinder 150×300 mm

FR-HSCC specimens

Fig. 6 Tensile strength of FR-SCC specimens before and after exposure to elevated temperatures
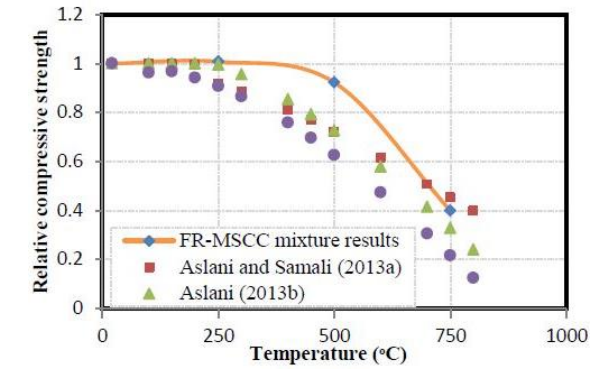

(a) Compressive strength

(b) Tensile strength

Fig. 7 Comparison between experimental results with proposed relationship for strength of SCC with different SF content at room temperature

temperature. However, some amount of divergence is observed regarding tensile strength of the specimens, especially in high strength ones. This result can be attributed to the type of fibers used. In this study, in addition to steel fiber, some amount of polypropylene fibers (PP) were added to the concrete mixture in order to prevent explosive spalling of specimens which will have been heated. Therefore the existence of PP made an extra contribution to the tensile strength of the specimens. Furthermore, the model were proposed based on much more steel fiber types having a variety of aspect ratio values most of which are higher than the aspect ratio of the steel fiber used in the current study (DRAMIX 3D 40/30).

When comparison between experimental and numerical results regarding strength values after elevated temperature are examined, there is acceptable agreement between them. Especially, there is a nearly perfect agreement between compressive strength results. Moreover the trend of change in tensile and compressive strengths are nearly same for experimental and numerical results.

According to the comparison it can be concluded that the model proposed by Aslani (2013b) works well for the prediction of compressive strength of both medium and high strength SCC specimens. Moreover, the model proposed by Aslani and Samali (2013b) has high correlation with the experimental results regarding compressive strength of high strength SCC specimens. The tensile strength results of high strength SCC specimens are very close to the corresponding values resulted from the study
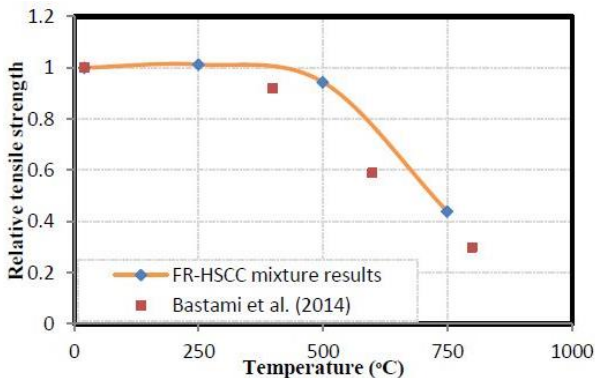
(a) FR-MSCC mixtures
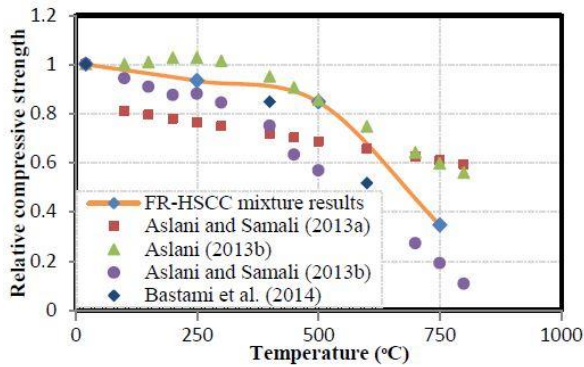
(b) FR-HSCC mixtures
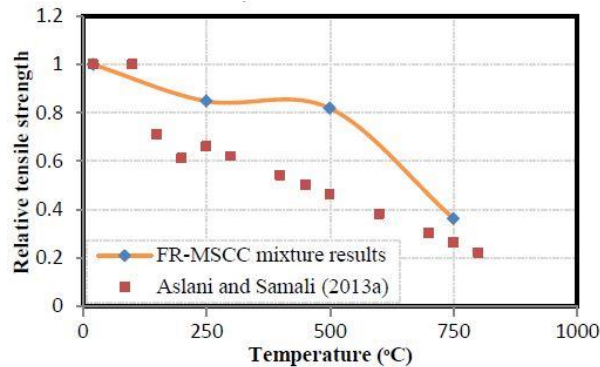
(c) FR-MSCC mixtures

(d) FR-HSCC mixtures

Fig. 8 Comparison between experimental results with proposed relationship for strength of concrete before and after exposure to elevated temperatures

carried out by Bastami *et al.* (2014), which is completely related with high strength concrete.

Table 8 Tensile strength of FR-HSCC specimens after exposure to different temperatures

Mixture	Specimen	Tensile strength at room temperature (MPa)	Residual strength (%) after exposure to elevated temperature		
			250°C	500°C	750°C
FR-HSCC-S0	S-100	**4.39**	121	84	43
	S-150	**4.3**	101	95	44
FR-HSCC-S5	S-100	**8.32**	81	77	38
	S-150	**8.18**	102	80	42
FR-HSCC-S10	S-100	**10.62**	78	63	39
	S-150	**9.15**	97	86	47

Due to existence of PP fibers in the specimens of the current study, there is some divergence between the experimental results and the proposed model by Aslani and Samali (2013b) regarding tensile strength values of medium strength SCC specimens. However, the reduction trend of the strength values with respect to temperature are similar for both results.

5. Theoretical analysis

5.1 Specimen size effect

5.1.1 The size effect law

The size effect law (SEL) is derived in this study by taking Bazant's theory (Bažant 1984) and fracture mechanics rules into account. Kim (1990) added a size independent strength term, $\sigma_o(=\alpha.f_{ct})$ to SEL and proposed a new formulation, called as modified size effect law (MSEL, Eq. (1)). The strength of concrete members can be predicted by the formulation even there are initial cracks and similar or dissimilar cracks in the members. Similar approach is also introduced by Bazant (1993) and Bažant and Xiang (1997) with a different method.

$$\sigma_N(d) = \frac{\beta.f_{ct}}{\sqrt{1 + \dfrac{d}{\lambda_\circ.d_a}}} + \alpha.f_{ct} \tag{1}$$

where $\sigma_N(d)$ represents the nominal strength, (f_{ct}) refers to the direct tensile strength, (d) is the characteristic dimension, (d_a) corresponds to the maximum aggregate size and (α, β, $\lambda_\circ$) represent the empirical constants. Although there are many studies related with size effect in concrete specimens about tensile failure and fracture properties (Kumar and Barai 2012), the size effect on compressive failure has not been sufficiently examined as compared to the tensile failure. Since concrete is mostly preferred construction material due to its perfect resistance to compressive forces, it is useful to extend the tensile size effect to size effect in the compressive failure mechanism. New and comprehensive equations are proposed by symbolic regression method. In these equations, the direct tensile strength term, (f_{ct}) used in MSEL equation is replaced by the compressive strength of standard cylinder
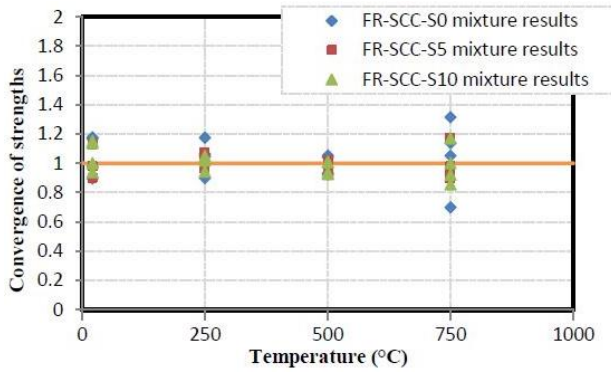
Fig. 9 Comparison between experimental and calculated compressive strength of FR-SCC cubes

(f_{cd}), and (λ_o) is an approximate constant whose value lies between 2.0 and 3.0 according to researchers (Bažant 1984, Kim *et al.* 2001). The value of 2.0 is used for the constant in regression analysis. The term (l_o) is used in the proposed equations and is equal to:

$$l_o = \lambda_o \times d_a = 2.0 \times d_a = 2.0 \times 11.0 = 22.0mm$$

where (d_a) is the maximum aggregate size used in SCC production, and equal to 11.0 mm for the present study.

5.1.2 Size effect on compressive strength
5.1.2.1 Cubic specimens
A new formulation (Eq. (2)) is proposed to calculate the

compressive strength of the cubic specimens in terms of standard strength for FR-SCC both with and without steel fiber, before and after exposure to elevated temperatures, by taking size effect into consideration. The correlation coefficient (R^2) of the equation is 0.894.

$$f_{cu} = \frac{0.76 f_K}{\sqrt{1 + \dfrac{d}{l_o}}} + 0.81 f_K \tag{2}$$

Where: $f_K = f_{cs} + \dfrac{R.I}{26.9} + \dfrac{T}{86.7}$

Where (f_{cu}) is the compressive strength (in MPa) of general cubic specimen, with or without steel fiber (SF) after exposure to different temperatures (T). As well, d is the cube dimension in cm, $l_o=2.0\times d_a$ and (d_a) is the maximum aggregate size. (f_{cs}) is the compressive strength of the standard specimen (S-150) in MPa for FR-MSCC or FR-HSCC mixtures. ($R.I$) is the fiber reinforcing index= $V_f \times \dfrac{l_f}{d_f}$, where (V_f) is the volume fraction of steel fiber, ($\dfrac{l_f}{d_f}$)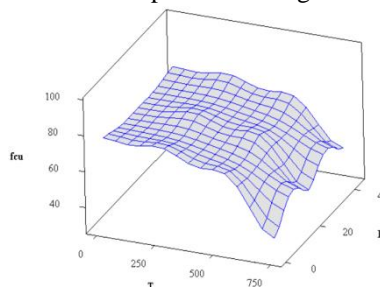 is the aspect ratio, (l_f and d_f) are the length and diameter of steel fiber, respectively, and (T) is the temperature in (°C). Fig. 9 compares the experimental and theoretical results of the compressive strength for FR-SCC
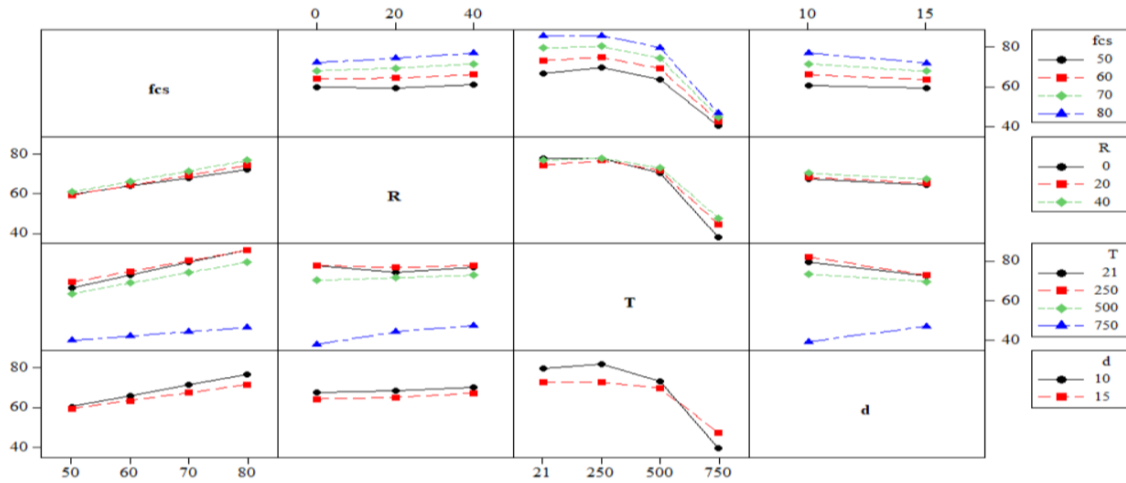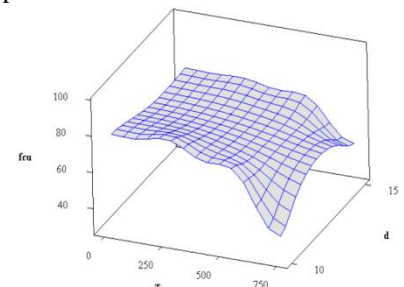

(a) Main effects on the compressive strength of cubic specimens
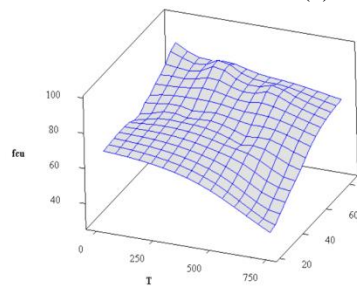
(b) Effect of standard strength on the compressive strength of cubes

(c) Effect the addition of fiber on the compressive strength of cubes

(d) Effect of specimen dimension on the compressive strength of cubes

Fig. 10 Size effect on compressive strength for FR-SCC cubes before and after exposure to elevated temperatures
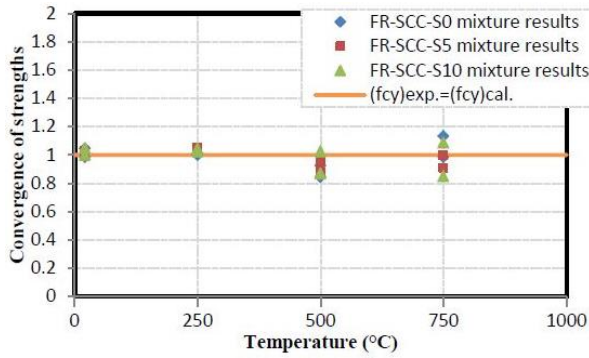
Fig. 11 Comparison between experimental and calculated compressive strength of FR-SCC cylinders

cubes.

Fig. 10 shows the main effects of variables in Eq. (2) on the compressive strength for cubic specimens of FR-SCC mixtures. As expected, size effect on the compressive strength of cubic specimens decreases with the increase in concrete grade, along with the addition of steel fibers, particularly when exposed to high temperatures. For temperature levels higher than 500°C, size effect on the residual strength of cubes was higher for larger cubes.

5.1.2.2 Cylindrical specimens

The proposed formulation to predict the compressive strength for different size of cylinders in terms of standard

strength of FR-SCC is given in Eq. (3). The correlation coefficient (R^2) in Eq. (3) was 0.973.

$$f_{cy} = \frac{f_L}{\sqrt{1 + \frac{d}{l_\circ}}} + 0.58 f_L \qquad (3)$$

Where: $f_L = f_{cs} + \frac{R.I}{97.4} - \frac{T}{245.3}$

(f_{cy}) is the compressive strength with the size of general cylinder, and (f_{cs}) the compressive strength of standard cylinder in MPa. The term "general" is used to specify any cylinder specimen that is concerned with various acceptable dimensions. A good fit between the experimental results and the results obtained from the proposed equations, as shown in Fig. 11.

Fig. 12 shows the interaction between the factors in Eq. (3), and their effects on the compressive strength of different cylindrical specimens of FR-SCC after different temperatures. This general compressive strength (f_{cy}) was a function of the standard strength (f_{cs}), fiber content, and temperature (T). The size effect on compressive strength of cylindrical specimens decreases with the concrete grade increase and/or after steel fiber addition.

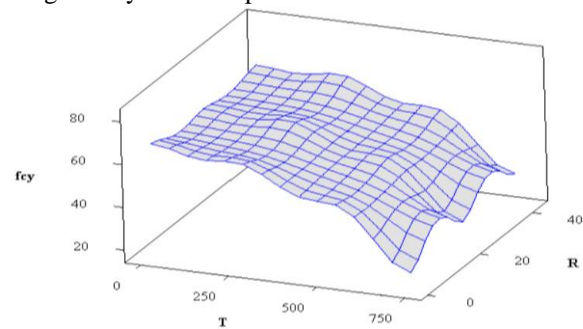### 5.1.3 Size effect on tensile strength

The proposed formulation obtained as a result of the regression analyses for the tensile strength results is given
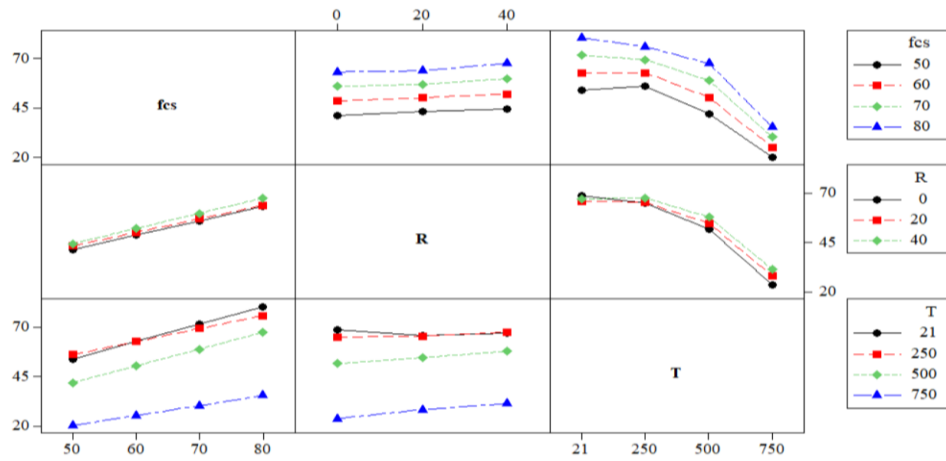
(a) Main effects on the compressive strength of cylindrical specimens
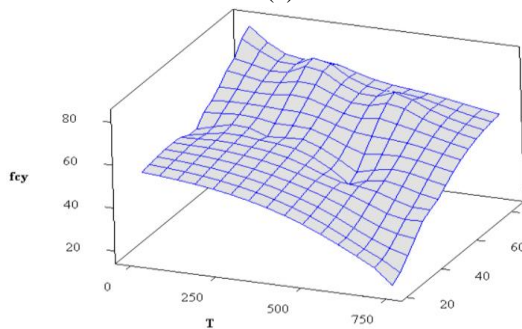
(b) Effect of standard strength on the compressive strength of cylinders

(c) Effect the addition of fiber on the compressive strength of cylinders

Fig. 12 Size effect on compressive strength for FR-SCC cylinders before and after exposure to elevated temperatures
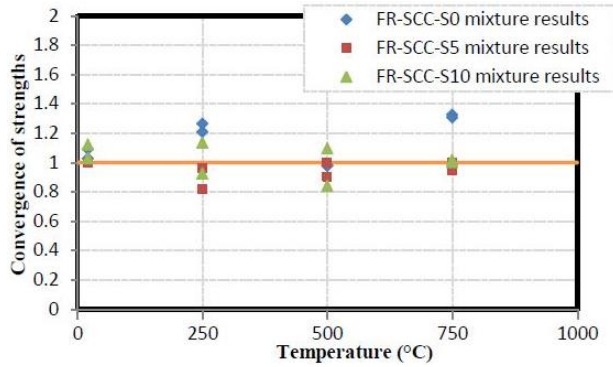
Fig. 13 Comparison between experimental and calculated tensile strength of FR-SCC cylinders

in Eq. (4). The tensile strength for different cylindrical specimens of FR-SCC mixtures after different temperatures can be obtained, in terms of the tensile strength of the standard cylinder practically with the proposed equation (Eq. (4)). The correlation coefficient R^2 was found to be 0.924.

$$f_t = \frac{87.5 f_M}{\sqrt{1 + \dfrac{d}{l_\circ}}} - 36.2 f_M \qquad (4)$$

Where: $f_M = f_{ts} + \dfrac{R.I}{118.7} - \dfrac{T}{1673}$

(f_t) is the tensile strength with the size of a general cylinder with or without steel fiber before and after exposure to

elevated temperatures, and (f_{ts}) is the tensile strength of standard cylinder in MPa. There was a clear convergence between the experimental and theoretical results of tensile strength as shown in Fig. 13.

Fig. 14 shows the main effects affecting on the general tensile strength of FR-SCC mixtures. From Eq. (4); the tensile strength for general size of the cylindrical specimens (f_t) was a function of standard tensile strength (f_{ts}) of FR-SCC (in MPa), steel fiber content, and temperature. In general, size effect on tensile strength increased with the temperature increasing, while decreases with the steel fibers addition and increase the concrete grade.

5.2 Specimen shape effect

Figs. 15 and 16 show the plots of compressive strength of the cylinders compared to the cubes, to represent the specimen shape effect. In these graphs, the dashed and solid lines show the lines of the highest fit achieved from linear regression analyses and the identity line ($Y=X$), respectively. The equations shown in Figs. 15 and 16 are obtained as a result of the linear regression analysis.

Comparing the compressive strength results of S-100 and C-100 specimens (see Figs. 15.a and 15.c), it can be seen that all trends show that the strength of C-100 specimens is higher than the strength of small cylinder (S-100) specimens for all concrete grades. Therefore, the difference between the strengths was approximately constant for all temperatures. However, the difference between the compressive strength of large cube (C-150) and small cylinder (S-100) decreased when the concrete grade increased, while it increased with higher temperatures, as
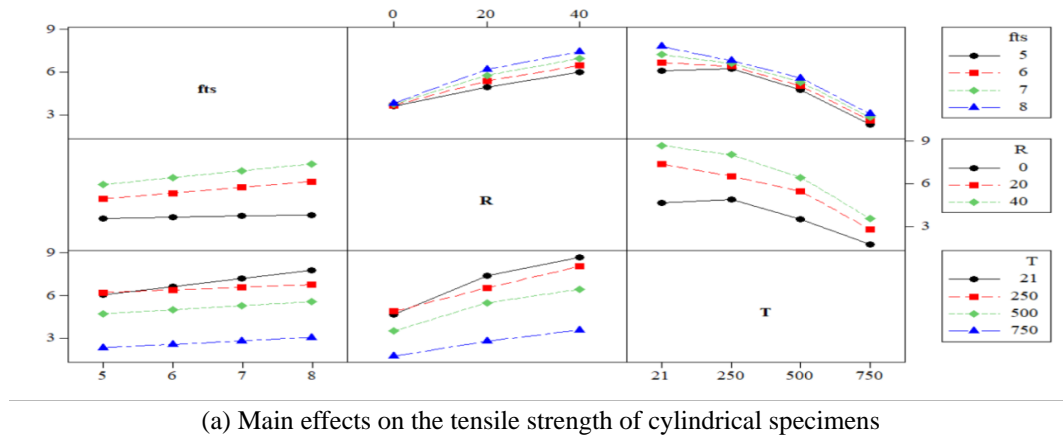
(a) Main effects on the tensile strength of cylindrical specimens
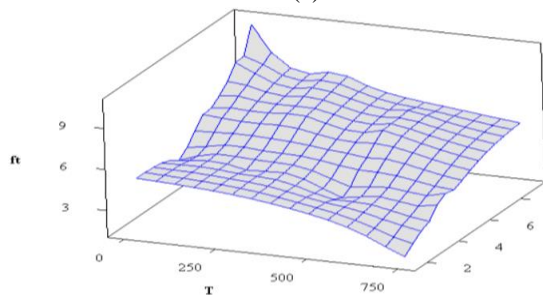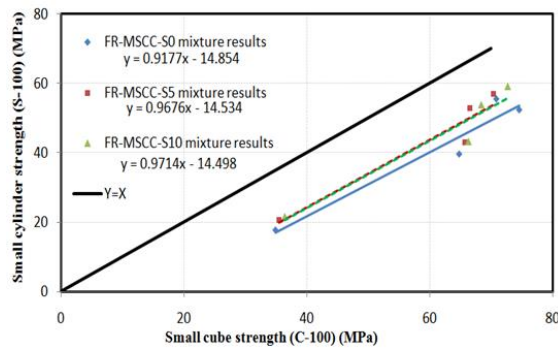

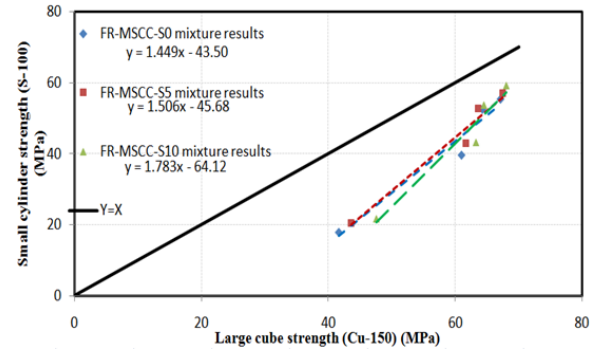(b) Effect of standard strength on the tensile strength of cylinders
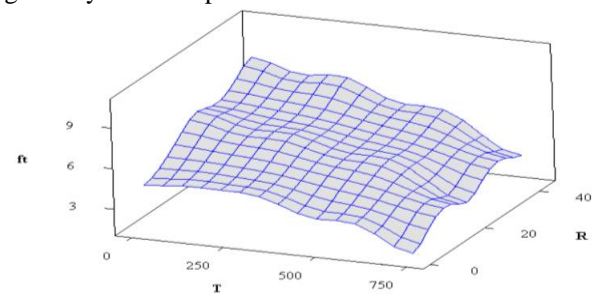
(c) Effect the addition of fiber on the tensile strength of cylinders

Fig. 14 Size effect on tensile strength for FR-SCC cylinders before and after exposure to elevated temperatures

(a) Cube 100 mm

(b) Cube 150 mm

FR-MSCC cubic specimens

(C) Cube 100 mm

(d)Cube 150 mm

FR-HSCC cubic specimens

Fig. 15 Relationship between compressive strengths of the 100×200 mm cylinder and cubic specimens before and after exposure to elevated temperatures
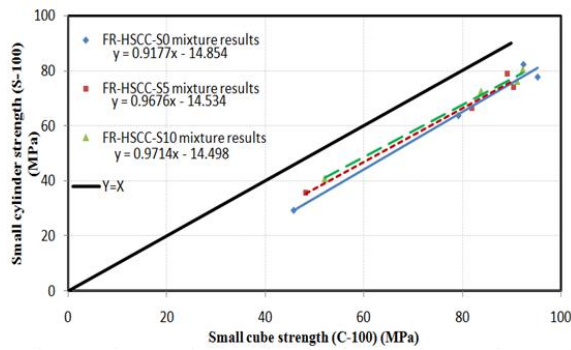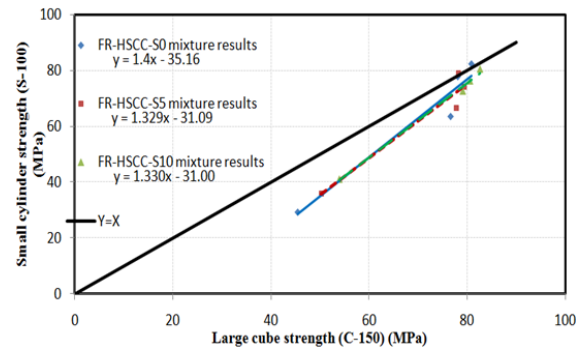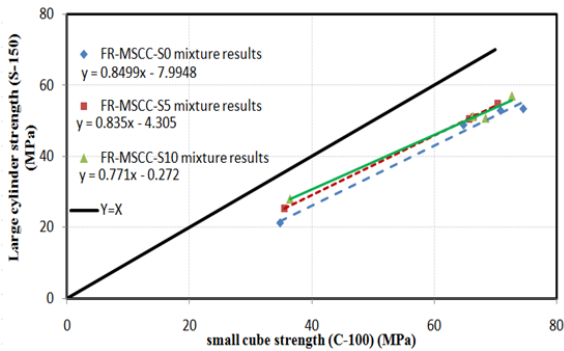

(a) Cube 100 mm

(b) Cube 150 mm
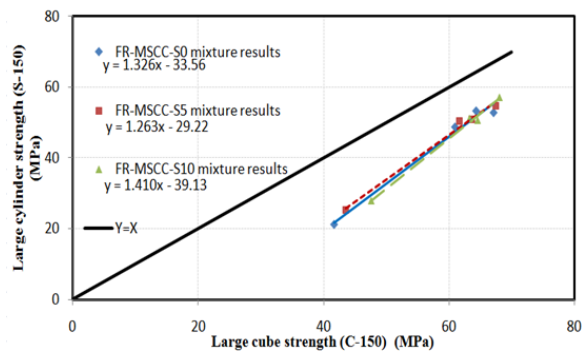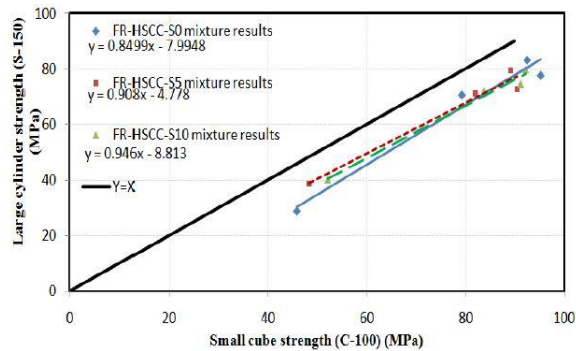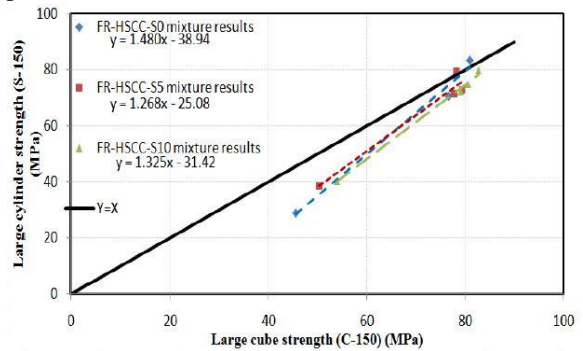
FR-MSCC cubic specimens
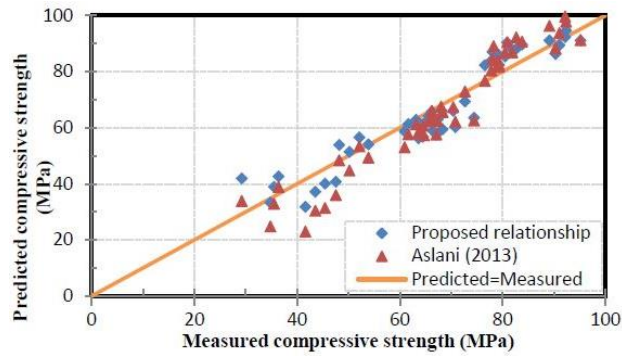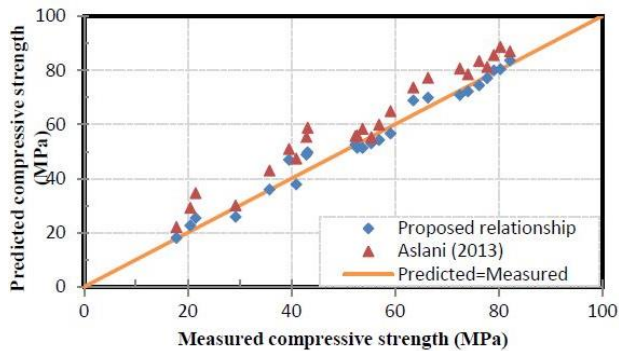
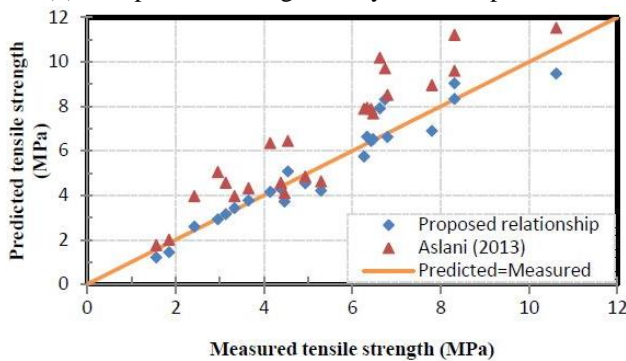(c) Cube 100 mm

(d) Cube 150 mm

FR-HSCC cubic specimens

Fig. 16 Relationship between compressive strengths of the 150×300 mm cylinder and cubic specimens before and after exposure to elevated temperatures

(a) Compressive strength for cubic specimens

(b) Compressive strength for cylindrical specimens

(c) Tensile strength for cylindrical specimens

Fig. 17 Comparison between measured and predicted strengths of FR-SCC specimens for the developed model and Aslani's model

shown in Figs. 15(b) and 16(d).

It can be concluded from Figs. 16 (b) and (d) that the difference in compressive strength for the large cube (C-150) and large cylinder (S-150) increased with the temperature increase or decrease the concrete grade for all SCC mixtures. Figs. 16(a) and 16(c) show that the compressive strength of the small cylinder (C-100) is higher than that of the large cylinder (S-150). The variance between these two specimens decreased when concrete grade increased or with steel fiber additions.

5.3 Verification of proposed model

Aslani (2013a) proposed some models to predict the size effect on the compressive and tensile strengths of the SCC. The fiber effect was also taken into consideration in these proposed models.

In the current study, new models were proposed, which are based on the model proposed by Aslani (2013a), by taking the temperature effect into account for SCC specimens with or without steel fiber. The standard specimen (S-150) was taken as reference for the production of the models. The f_{cs} term in Eqs. (2)-(3) represents the compressive strength of the standard specimen at concerning temperature. Similarly, f_{ts} in Eq. (4) represents the tensile strength of the standard specimen at relevant temperature. Except insertion of temperature effect, all remaining operations of the proposed procedure is similar with the literature, especially with the procedure proposed by Aslani (2013a). Since the reference strength values (f_{cs} and f_{ts}) are determined according to the temperature which is point of concern, the results of the developed model is based on actual residual strength values of corresponding temperature instead of the predicted value of the residual strength. This situation increases the reliability and accuracy of the developed model of the current study.

The present developed models are compared with those proposed by Aslani (2013a) as shown in Fig. 17. There is a slight difference between two models. The reason is that the effect of temperature is taken into account in the present models. It can be concluded from Fig. 17 that the model proposed by Aslani (2013a) works well for the prediction of the size effect on the compressive strength of SCC specimens even for high temperatures, especially up to 500 ^{o}C (R^2=0.84 and 0.91 for cubic and cylindrical specimens, respectively). However, since the effect of steel fiber is much more apparent in tensile strength, accuracy of the model declines slightly for the tensile strength of SCC specimens which are heated. The developed models can be used effectively in order to find the size effect on both compressive and tensile strengths of different specimen types of SCC with and without SF (R^2=0.89 and 0.97 for compressive strengths of cubic and cylindrical specimens, respectively. R^2=0.92 for tensile strengths of cylindrical specimens). Furthermore, the developed model works for both room temperature and elevated temperature.

6. Conclusions

In this study, different size and shape of specimens of fiber reinforced self-compacting concrete (FR-SCC) were produced with two concrete grades (medium and high) and exposed to elevated temperatures up to 750℃. Size effect on residual compressive and tensile strengths of heated specimens were studied. Moreover, new and practical formulations were proposed to obtain the compressive strength for the cubic and cylindrical specimens, and tensile strength for cylindrical specimens of FR-SCC before and after exposure to elevated temperature. Since the formulations are based on fracture mechanics, the compressive strength of the standard cylinder, steel fiber content, and temperature terms were taken into consideration. Based on the experimental and analytical work, the following conclusions are drawn:

• Considering the fresh SCC test results, the addition of fibers decreases the workability of SCC.
• Provision of polypropylene fibers can prevent SCC

from explosive spalling and the addition of steel fibers improves the residual strength of FR-SCC specimens subjected to elevated temperatures.

• Cubic specimens can retain considerably higher compressive strength as compared to cylinder specimens after exposure to high temperatures. Also, the temperature effect on 150 mm cube was the least as compared to other specimens (cylinders and cubes).

• Performance of cubic specimens with steel fibers was the most efficient. However, the residual compressive strength of cubic specimens is higher than that of the cylindrical specimens. Therefore, the preference of the cubic shaped structural element can be more reliable when the risk of high temperature is concerned.

• Size effect on the conversion factor difference is lower for greater concrete grades. Addition of steel fiber to SCC mixtures, on the other hand, causes a reduction in temperature effect on the variation of a conversion factor.

• Reduction in tensile strength of small cylinders is quicker as compared to that of large cylinder after exposure to elevated temperatures. Therefore, tensile strength results of the standard size cylinder are more reliable than cylinder specimens with other sizes.

• High prediction accuracy of proposed models confirms that the equations can be used safely to predict the strength values for different specimens of fiber-reinforced self-compacting concrete subjected to high temperatures.

• Generalization capability of proposed formulations is high for both compressive and tensile strength calculations, which enables the designers to use the formulations for all types of SCC (medium or high strength, with or without steel fiber).

• It is concluded that the results of the experimental study are compatible with the corresponding proposed numerical models in literature generally. Moreover, the developed model for the size effect in the current study exhibits high agreement with the previously proposed models which take only room temperature into consideration.

References

Aslani, F. (2013a), "Effects of specimen size and shape on compressive and tensile strengths of self-compacting concrete with or without fibres", *Mag. Concrete Res.*, **65**(15), 914-929.

Aslani, F. (2015a), "Nanoparticles in self-compacting concrete-a review", *Mag. Concrete Res.*, **67**(20), 1084-1100.

Aslani, F. (2013b), "Prestressed concrete thermal behaviour", *Mag. Concrete Res.*, **65**(3), 158-171.

Aslani, F. (2015b), "Thermal performance modeling of geopolymer concrete", *J. Mater. Civil Eng.*, **28**(1), 4015062.

Aslani, F. and Bastami, M. (2011), "Constitutive relationships for normal- and high-strength concrete at elevated temperatures", *ACI Mater. J.*, **108**(4), 355-364.

Aslani, F. and Bastami, M. (2015), "Relationship between deflection and crack mouth opening displacement of self-compacting concrete beams with and without fibers", *Mech. Adv. Mater. Struct.*, **22**(11), 956-967.

Aslani, F. and Maia, L. (2013), "Creep and shrinkage of high-

strength self-compacting concrete : experimental and analytical analysis", *Mag. Concrete Res.*, **65**(17), 1044-1058.

Aslani, F., Maia, L. and Santos, J. (2017), "Effect of specimen geometry and specimen preparation on the concrete compressive strength test", *Struct. Eng. Mech.*, **62**(1), 97-106.

Aslani, F. and Natoori, M. (2013), "Stress-strain relationships for steel fiber reinforced self- compacting concrete", *Struct. Eng. Mech.*, **46**,(2), 295-322.

Aslani, F. and Nejadi, S. (2013), "Mechanical characteristics of self-compacting concrete with and without fibres", *Mag. Concrete Res.*, **65**(10), 608-622.

Aslani, F. and Samali, B. (2013a), "Constitutive relationships for self-compacting concrete at elevated temperatures", *Mater. Struct.*, **48**(1-2), 337-356.

Aslani, F. and Samali, B. (2013b), "Predicting the bond between concrete and reinforcing steel at elevated temperatures", *Struct. Eng. Mech.*, **48**(5),643-660.

ASTM Standards (2004), *Standard Test Method for Compressive Strength of Cylindrical Concrete Specimens*, Annual Book of ASTM Standards (ASTM C39-01), American Society for Testing and Materials, Philadelphia, USA.

Bamonte, P. and Gambarova, P.G. (2016), "High-temperature behavior of SCC in compression: comparative study on recent experimental campaigns", *J. Mater. Civil Eng.*, **28**(3), 4015141.

Bastami, M., Baghbadrani, M. and Aslani, F. (2014), "Performance of nano-Silica modified high strength concrete at elevated temperatures", *Constr. Build. Mater.*, **68**, 402-408.

Bazant, Z.P. (1993), "Size effect in tensile and compressive quasibrittle failures.", *JCI International Workshop on Size Effect in Concrete Structures*, 141-160.

Bažant, Z.P. (1984), "Size effect in blunt fracture: concrete, rock, metal", *J. Eng. Mech.*, **110**(4), 518-535.

Bažant, Z.P. and Xiang, Y. (1997), "Size effect in compression fracture: splitting crack band propagation", *J. Eng. Mech.*, **123**(2), 162-172.

B.S (2000). *Testing Hardened Concrete: Compressive Strength of Test Specimens,* British Standard Institution, London, U.K.

Dehestani, M., Nikbin, I.M. and Asadollahi, S. (2014), "Effects of specimen shape and size on the compressive strength of self-consolidating concrete (SCC)", *Constr. Build. Mater.*, **66**, 685-691.

Dias, W.P.S., Khoury, G.A. and Sullivan, P.J.E. (1990), "Mechanical properties of hardened cement paste exposed to temperatures up to 700 C (1292 F)", *Mater. J.*, **87**(2), 160-166.

EFNARC (2005), *The European Guidelines for Self-Compacting Concrete, Specification, Production and Use*, Experts for Specialised Construction and Concrete Systems, Farnham, UK.

Fares, H., Remond, S., Noumowe, A. and Cousture, A. (2010), "High temperature behaviour of self-consolidating concrete: microstructure and physicochemical properties", *Cement Concrete Res.*, **40**(3), 488-496.

Kim, J.K. (1990), "Size effect in concrete specimens with dissimilar initial cracks", *Mag. Concrete Res.*, **42**(153), 233-238.

Kim, J.K., Yi, S.T. and Kim, J.H.J. (2001), "Effect of specimen sizes on flexural compressive strength of concrete", *Struct. J.*, **98**(3), 416-424.

Kourkoulis, S.K. and Ganniari-Papageorgiou, E. (2010), "Experimental study of the size-and shape-effects of natural building stones", *Constr. Build. Mater.*, **24**(5), 803-810.

Kumar, S. and Barai, S.V. (2012), "Size-effect of fracture parameters for crack propagation in concrete: a comparative study", *Comput. Concrete*, **9**(1), 1-19.

Maia, L. and Aslani, F. (2016), "Modulus of elasticity of concretes produced with basaltic aggregate", *Comput. Concrete*, **17**(1), 129-140.

Nikbin, I.M., Dehestani, M., Beygi, M.H.A. and Rezvani, M.

(2014), "Effects of cube size and placement direction on compressive strength of self-consolidating concrete", *Constr. Build. Mater.*, **59**, 144-150.

Sideris, K.K. (2007), "Mechanical characteristics of self-consolidating concretes exposed to elevated temperatures", *J. Mater. Civil Eng.*, **19**(8), 648-654.

Sim, J.I., Yang, K.H., Kim, H.Y. and Choi, B.J. (2013), "Size and shape effects on compressive strength of lightweight concrete", *Constr. Build. Mater.*, **38**, 854-864.

Del Viso, J.R., Carmona, J.R. and Ruiz, G. (2007), "Size and shape effects on the compressive strength of high strength concrete", *Proceedings of the 6th International Conference on Fracture Mechanics of Concrete and Concrete Structures*, 1297-1304.

Van Der Vurst, F., Desnerck, P., Peirs, J. and De Schutter, G. (2014), "Shape factors of self-compacting concrete specimens subjected to uniaxial loading", *Cement Concrete Compos.*, **54**, 62-69.

Yi, S.T., Yang, E.I. and Choi, J.C. (2006), "Effect of specimen sizes, specimen shapes, and placement directions on compressive strength of concrete", *Nucl .Eng. Des.*, **236**(2), 115-127.

Zhang, B. and Bicanic, N. (2002), "Residual fracture toughness of normal-and high-strength gravel concrete after heating to 600 C", *Mater. J.*, **99**(3), 217-226.

HK

Notations

$\sigma_N(d)$	is the nominal strength (in MPa).
d	is the dimension of the specimen (in cm).
f_{ct}	is the direct tensile strength (in MPa).
α, β, λ_o	are the empirical constant.
f_{cu}	is the compressive strength with the size of the general cube for FR-SCC with or without steel fiber before and after exposure to elevated temperature (in MPa).
f_{cs}	is the compressive strength of the standard cylinder with the size of 150×300 mm for FR-SCC with or without steel fiber before and after exposure to elevated temperature (in MPa).
d_a	is the maximum aggregate size (in mm).
$R.I$	is the fiber reinforcing index.
V_f	is the volume fraction of steel fiber (%).
d_f	is the diameter of steel fiber (in mm).
l_f	is the length of steel fiber (in mm).
T	is the temperature degree (℃).
f_{cy}	is the compressive strength with the size of the general cylinder for FR-SCC with or without steel fiber before and after exposure to elevated temperature (in MPa).
f_t	is the tensile strength with the size of the general cylinder for FR-SCC with or without steel fiber before and after exposure to elevated temperature (in MPa).
f_{ts}	is the tensile strength of the standard cylinder with the size of 150×300mm for FR-SCC with or without steel fiber before and after exposure to elevated temperature (in MPa).